Fall 12-14-2018

SYNTHESIS OF DOXORUBICIN-BASED PRODRUG AND ACTIVATABLE MR NANOPROBE FOR THE IMAGING AND TREATMENT OF CANCER

Bayan Dous
Pittsburg State University, bdous@gus.pittstate.edu

SYNTHESIS OF DOXORUBICIN-BASED PRODRUG AND ACTIVATABLE MR NANOPROBE FOR THE IMAGING AND TREATMENT OF CANCER

A thesis submitted to the Graduate School
In Partial Fulfillment of the Requirements For
the Degree of Master of Science in Chemistry

Bayan Ahmad S Dous

Pittsburg State University

Pittsburg, Kansas

November 2018

SYNTHESIS OF DOXORUBICIN-BASED PRODRUG AND ACTIVATABLE MR NANOPROBE FOR THE IMAGING AND TREATMENT OF CANCER

Bayan Ahmad S Dous

APPROVED:

Thesis Advisor _____
Dr. Santimukul Santra, Department of Chemistry

Committee Member _____
Dr. Irene Zegar, Department of Chemistry

Committee Member _____
Dr. Dilip Paul, Department of Chemistry

Committee Member _____
Dr. Cynthia Huffman, Department of Mathematics

ACKNOWLEDGMENTS

I would like to express my special thanks to my advisor and mentor in my thesis Dr. Santimukul Santra, who gave me the golden opportunity to work on this project. This work would not have been possible without his guidance.

I would like to thank the Saudi Arabia Cultural Mission (SACM) for giving me this great opportunity to be here and study abroad.

Also, I want to thank my lab members for their wonderful collaboration. They supported me greatly and were always willing to help me. Thanks for them for their friendship in the lab.

To my mother Wafaa and my father Ahmad; this work is for them and to make them proud. They supported me, believed in my potential, and surrounded me with prayers all the time. They are my ultimate role models.

Thanks to my friends who were for me. They were with me in the difficulties and extremely supported me

SYNTHESIS OF DOXORUBICIN-BASED PRODRUG AND ACTIVATABLE MR NANOPROBE FOR THE IMAGING AND TREATMENT OF CANCER

An Abstract of the Thesis by
Bayan Ahmad S Dous

Magnetic Resonance Imaging (MRI) is increasingly being used as a diagnostic tool for cancer. We propose a novel molecular probe, Gadolinium-DTPA disulfide-bonded Doxorubicin (Gd-DTPA-SS-Doxo) encapsulated in iron oxide which could provide a dual modality for detecting malignant growth while simultaneously targeting treatment options. We first synthesized Gd-DTPA-SS-Doxo followed by encapsulation within the poly (acrylic acid) (PAA) coating of iron oxide nanoparticle (IONP), producing a nanoprobe (IO-Gd-DTPA-SS-Doxo) with quenched longitudinal spin lattice magnetic relaxation (T1). After receptor-mediated internalization, Gd-DTPA-SS-Doxo is released from the nanoprobe's polymeric coating due to the acidic microenvironment of the tumor. When the molecular probe is subjected to various enzymes present in the cancerous cells, the disulfide bond of the molecular probe is cleaved. This results in an intracellular release of Gd-DTPA complex and Doxo with subsequent T1 activation and cytotoxic effect respectively. Therefore, the proposed framework would give dual mode MR imaging of malignant growth, target ability and treatment for disease.

TABLE OF CONTENTS

CHAPTER **PAGE**

LIST OF TABLES

TABLE **PAGE**

LIST OF FIGURES

FIGURE **PAGE**

LIST OF SCHEMES

SCHEME **PAGE**

LIST OF ABBREVIATIONS

IONPs: Iron Oxide nanoparticles

PAA: Poly (acrylic acid)

IONP-COOH: Carboxylated iron oxide nanoparticles

IONP-FOL: Folate conjugated iron oxide nanoparticles

EDC/NHS: 1-ethyl-3-(3-dimethylaminopropyl) carbodiimide)

DLS: Dynamic light scattering

DMSO: Dimethyl sulfoxide

MTT: (3-(4, 5-dimethyl-thiazol-2-yl)-2, 5 diphenyl tetrazolium bromide)

NHS: N-hydroxy succinimide

LNCaP cells: Lymph Node Carcinoma of Prostate Cancer cells

PBS: Phosphate buffer saline

DTPA: diethylenetriaminepentaacetic acid

GSH: Glutathiol

MALDI-TOF: Matrix-assisted laser desorption/ionization

CHAPTER I

SYNTHESIS OF DOXORUBICIN-BASED PRODRUG AND ACTIVATABLE MR NANOPROBE FOR THE IMAGING AND TREATMENT OF CANCER

INTRODUCTION

Cancer is presently the second most basic reason for death in the U.S. As indicated by the American Cancer Society[1] prostate cancer is anticipated to cause roughly 12 million deaths by 2030 [1], 164,690 new cases are expected in 2018, and 29,430 estimated deaths. Because of those huge numbers, scientists are focusing their studies trying to find a way to fight this disease. Currently practiced techniques such as radiation, surgery, hormone therapy, and chemotherapy are known to cause harm and damage to the healthy cells, risking the patients' survival [2]. For this reason; in 1980s, as an attempt to decrease the damage to healthy cells, scientists worked with nanoparticles (NPs), which were designed to target only the cancer cells [2]. Considering the severity of prostate cancer, this work will focus on the development of magnetic nanotheranostics for the imaging and treatment of this cancer.

Magnetic Resonance Imaging (MRI) is a technique employed in tissue imaging and clinical diagnosis of diseases. It permits visualization of tissues and organs, and also makes it possible to regenerate noninvasive sectional images[3]. In other words, molecular imaging techniques facilitate pathologic biomarker detection, thus, enhancing diagnosis of diseases and improved therapeutic management [3, 4, 6]. MRI has gained significant attention in the field of molecular imaging due to its numerous benefits, including short imaging times, high spatial resolution (µm-scale), impressive signal-to-noise (S/N) ratio, and its noninvasive characteristics [6]. Biological processes, such as accumulation of lipids and angiogenesis signal the early development of some clinical conditions, are widely targeted by MRI contrast agents [4]. In addition, MRI contrast agents target conditions, such as plaque rupture-induced tissue factors and fibrins; bio signatures that occur later. These contrast agents combine the benefits of therapeutic intervention and disease diagnosis since they can be used as vehicles for drug delivery [6]. MRI contrast agents are essential requisites in distinguishing healthy tissues from infected ones. Water is the primary constituent of living tissues; MRI primarily targets protons in the water by exciting and detecting any changes in their rotational motion and direction [7].

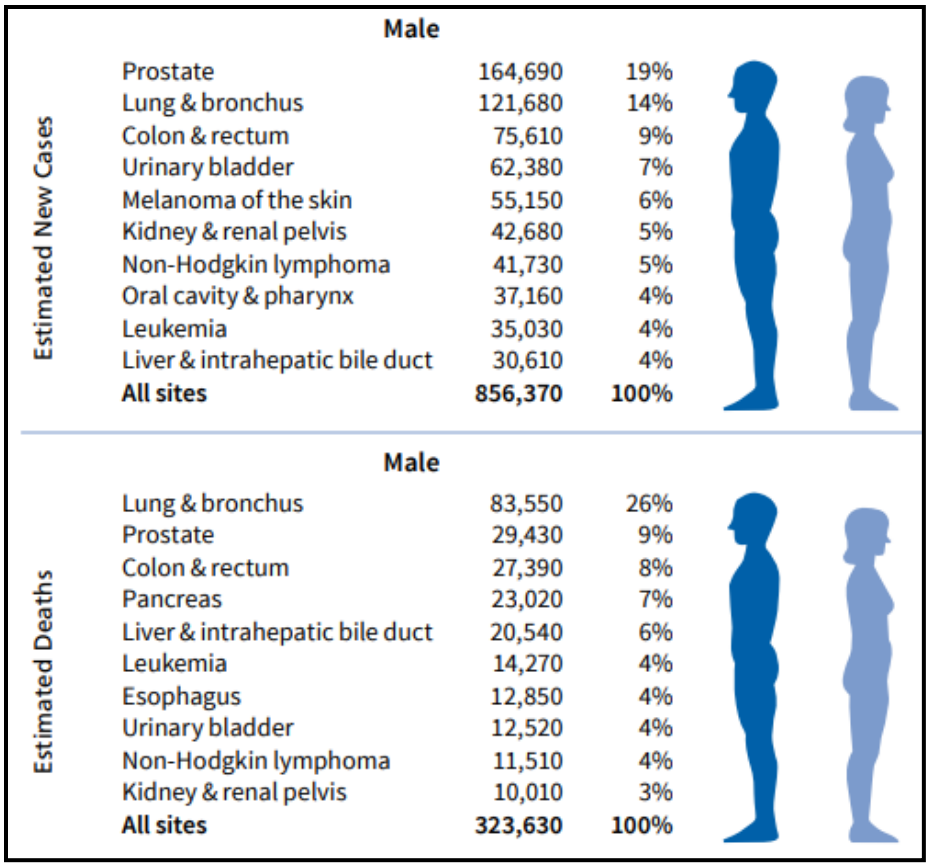

Male

Estimated New Cases

Prostate	164,690	19%
Lung & bronchus	121,680	14%
Colon & rectum	75,610	9%
Urinary bladder	62,380	7%
Melanoma of the skin	55,150	6%
Kidney & renal pelvis	42,680	5%
Non-Hodgkin lymphoma	41,730	5%
Oral cavity & pharynx	37,160	4%
Leukemia	35,030	4%
Liver & intrahepatic bile duct	30,610	4%
All sites	**856,370**	**100%**

Male

Estimated Deaths

Lung & bronchus	83,550	26%
Prostate	29,430	9%
Colon & rectum	27,390	8%
Pancreas	23,020	7%
Liver & intrahepatic bile duct	20,540	6%
Leukemia	14,270	4%
Esophagus	12,850	4%
Urinary bladder	12,520	4%
Non-Hodgkin lymphoma	11,510	4%
Kidney & renal pelvis	10,010	3%
All sites	**323,630**	**100%**

Figure 1: Leading Sites of New Cancer Cases and Deaths – 2018 Estimates[1].

In practice, the water content in the tissues and the longitudinal rate of relaxation, R_1 (in terms of 1/sec.), are proportional to the MRI signal; R_1 describes the relaxation rate of the MRI signal during pulse sequencing [4]. The protons in the body tissues are realigned with the magnetic field. An MRI scan stimulates the protons, which shift from equilibrium. From this excited state there are two forms of relaxation. The most rapid form of relaxation is the dephasing of the spins, this is known as T2 relaxation or transverse relaxation. This has the effect of reducing the overall magnetization vector in the XY plane. The second slower form of relaxation involves the return to equilibrium of spin up and spin down states, this is known as T1 relaxation or longitudinal relaxation. This has the

effect of restoring the overall magnetization vector in the Z direction. Such magnetic features make it possible to differentiate tissues [8].

The polymer-coated iron oxide nanoparticles (IONPs) are polymer-coated and superparamagnetic, which are used to enhance the contrast of tomographic MR images from disease site and organs. The polymeric coating enhances the stability of IONPs in aqueous media[9]. IONPs decrease the MR signal (dark, negative contrast) of an MRI sequence that is T_2-weighted, by reducing the transverse time of relaxation time T2 of the neighboring protons [11]. So far, IONPs have proven to be the most desirable superparamagnetic agents in improving the contrast in T2 MR Scans. The choice of IONPs is often acknowledged by their minimal toxicity to cancer cells [5].

Gadolinium complex (Gd-DTPA) is a paramagnetic metal chelate used as a MRI contrast agent. Its principle role is to reduce the water protons' longitudinal time of relaxation, T_1, thus enhancing the intensity of T_1-weighted images (bright, positive contrast), which can be visualized by a radiologist [12]. Gd-DTPA contrast agent comprises atoms and molecules that are closely-packed by strong chemical bonds between the chelating agent (DTPA) and Gd^{3+}. Due to the high toxicity of Gd^{3+}, the ions are often coupled with a chelating agent ensuring the magnetic property is retained. During a MRI scan, the contrast agent is injected into a tissue and subsequently removed from the human body through the kidneys.

The formulation of Gd-DTPA (diethylenetriamine pentaacetic acid) is essentially an activatable MRI nanoprobe encapsulated within an IONP to obtain a composite nanoprobe. In nanomedicine, both MRI contrast agents can be utilized in dual mode, as Gd-IONP. When exposed to acidic environments, the composite contrast agent is activated, thus, enhancing the T_1 weighted signal (brighter contrast). The Fe_2O_3 core comprises magnetically-ordered pairs of Fe^{2+} and Fe^{3+} ions within the nanocrystal [9]. The net magnetic moment exerted by the combination exceeds that of the single paramagnetic Gd^{3+}, Fe^{2+} and Fe^{3+}. In tandem, it is expected that the magnetic core will become susceptible to the intense magnetic moment created and subsequently, affect Gd-DTPA's time of relaxation, T_1. Further, it is expected that the composite magnetic nanoprobe will relax at a rate of $1/T_1$ when the Gd-DTPA complex is extracted from the polymeric coating of the nanoprobe to elicit dequenching [9].

Many studies have been conducted over time and in one study (**Scheme 1**) they reported a synthesis of an activatable prodrug (Doxo-SS-Fol), and also a nonactivatable probe (Doxo-CC-Fol) [13]. They observed that due to a high GSH level in cancer cells the disulfide bond was cleaved leading to the activation of fluorescence emission and cytotoxicity. On the other hand, it remains OFF when a non-activatable drug was introduced because of the absence of the cleaving mechanism.

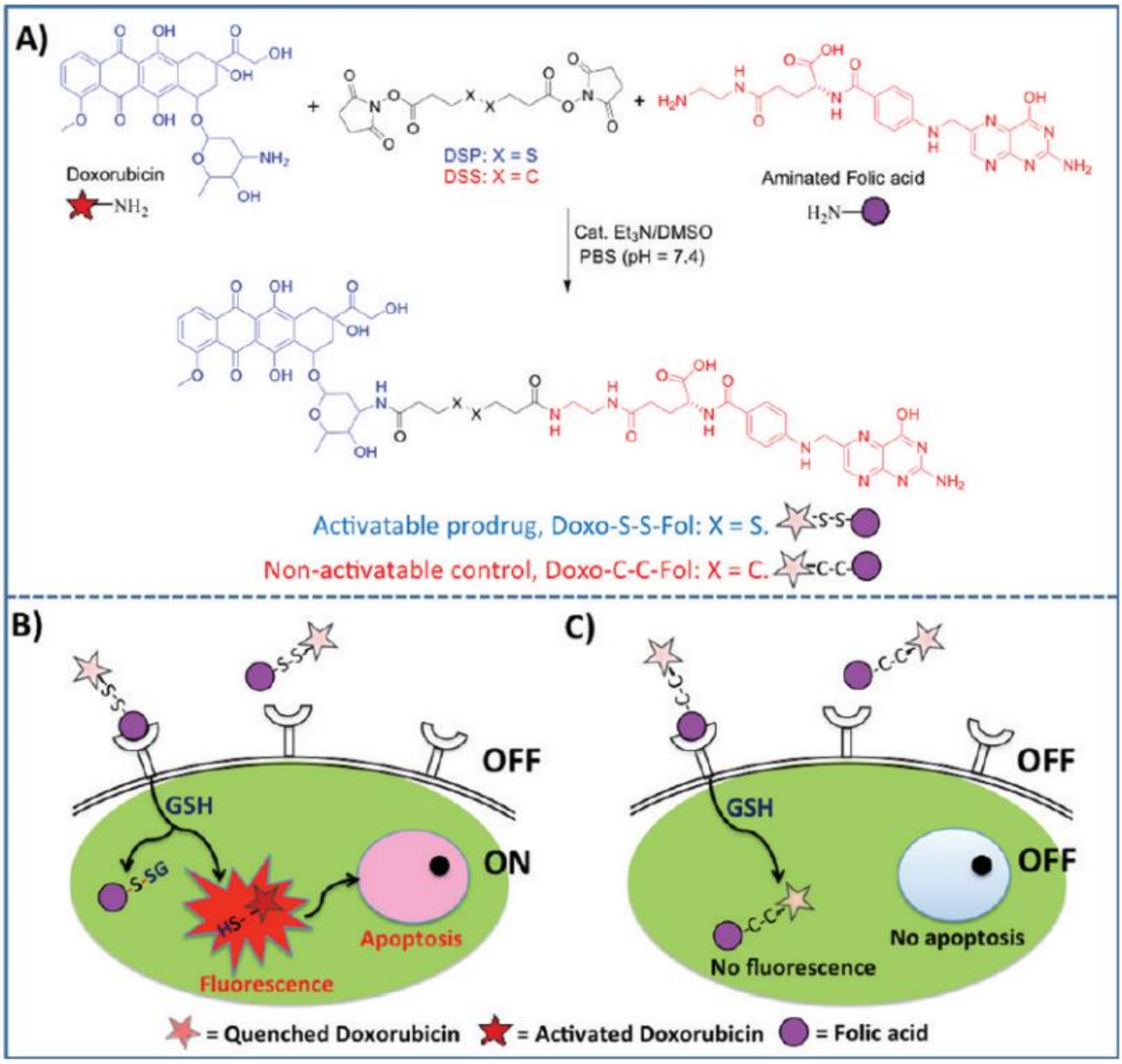

Scheme 1: Doxorubicin-based activatable prodrug for the targeted treatment of lung cancer[13].

To track the final localization of the prodrug cells, the presence of the folate receptor and the final localization of the conjugate in cultured cells, many folate conjugation with nanoparticles and fluorescent dyes have been developed and used [13]. In (**Scheme 1B**), it was found that when the prodrug is linked with carbon-carbon covalent bond; the fluorescence and cytotoxicity of the

doxorubicin are quenched (OFF). on the other hand, it became activated (ON) when the linkage is done with a disulfide bond (S-S), dithiobis (succinimidyl propionate) (DSP) were in the design of the conjugation (**Scheme 1A**); linking the cytotoxic doxorubicin and the targeting folate unit. So, upon interaction and by using a specific enzyme associated with disease, an activatable molecular imaging agent becomes activated; an increase was noticed in its signal output[14]. This allows the lower signal background and the image resolution to increase. In the meantime, when the prodrug is less toxic it enters the sick cells and became active [13]. In this study, the folic acid can act as both a quencher for the doxorubicin and a receptor targeting ligand (**Scheme 1**).

In the study[15], they designed the prodrug Lac-SS-DCM created with a disulfide bond unit and an alkyne reaction group. It reduces the side effects and gives higher anticancer effectiveness as well as excellent target ability. The multivalent galectin-targeting ligand was performed when lactose-mediated endocytosis resulting from the surface lactose corona[15]. The quenching of the strong NIR fluorescence light of the compound Lac-SS-DCM was done via the newly formed amide bond. In addition, taking advantage of the disulfide bond (-SS-) the prodrug causes disband by the enzyme (GSH), which makes the drug to be active inside the cancer cells[15] (**Scheme 2**).

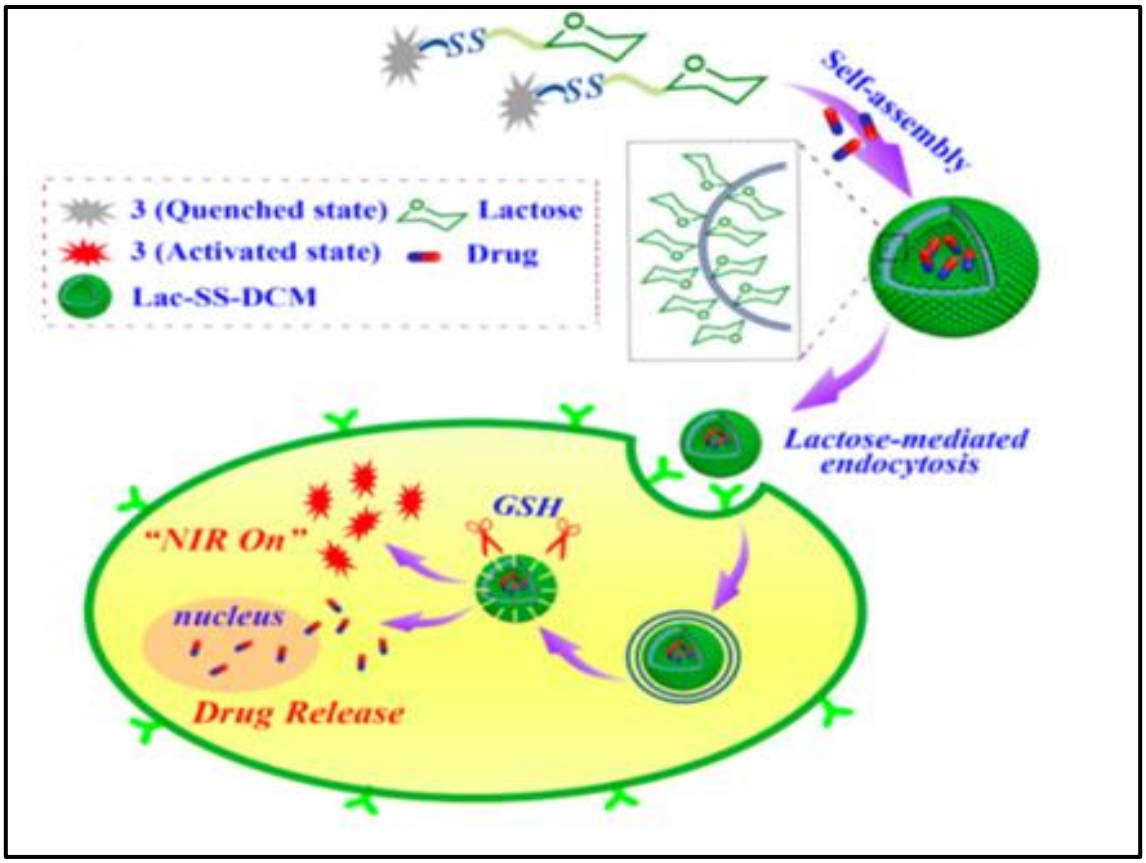

Scheme 2: Prodrug Lac-SS-DCM[15] for the treatment of cancer.

In a different study[16], they provide a design with multimodal probe which was very active tool for repaid and giving the imaging of the biological steps. This special design can show multiplex imaging signals due to the interaction with the specific molecules in the design. They studied and reported that the design follows a stimuli-responsive disassembly approach and has three sides as shown in (**Scheme 3**).

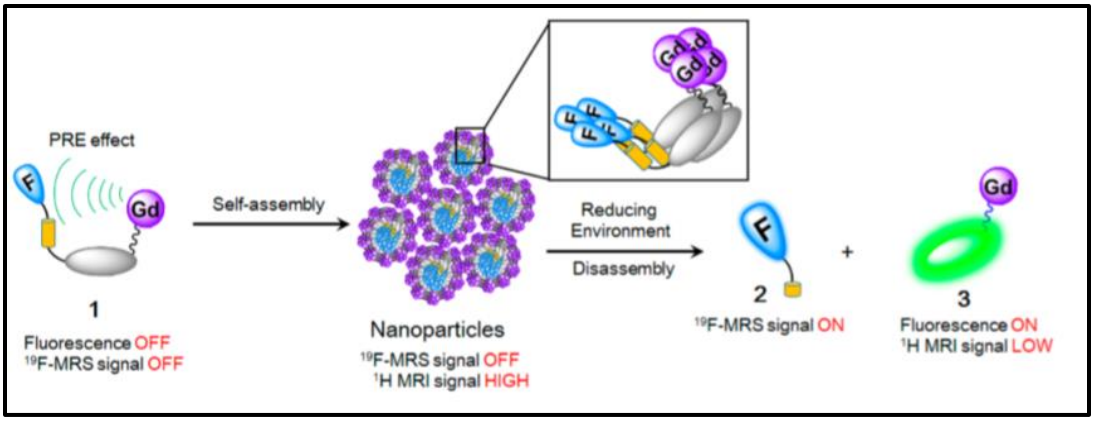

Scheme 3: The concept behind the design of an activatable probe[16].

Santra e t. al., developed novel activatable MR probe by encapsulating Gd-DTPA complex in iron oxide nanoparticles (IONPs) for the imaging and treatment of cancer[5]. It was found that the Gd's T1 MR contrast was dequenched (activated) after releasing the Gd-DTPA complex inside the cancer cells, facilitating for an activatable T1 MR images for diagnosis[5].

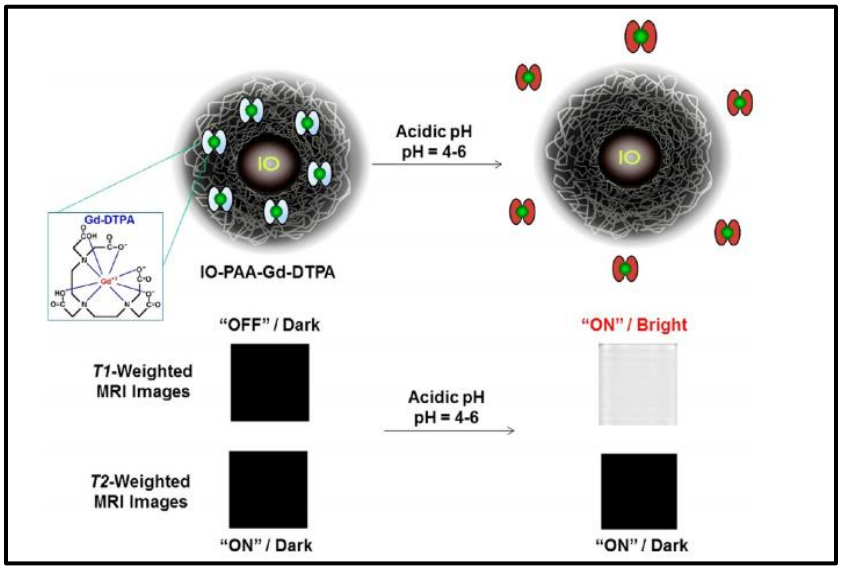

Scheme 4: composite magnetic nanoprobe IO-PAA-Gd-DTPA and corresponding T1 MR Activation[5].

The aim of this study is to utilize the Gd-DTPA and IONPs (Fe^{2+} + F^{3+}) carrier molecules as a dual mode MRI nanoprobe for treatment and imaging of cancer. In this study (**Scheme 5A**), we are proposing a Doxo-SS-Gd-DTPA nanoprobe encapsulating IONPs for the MR imaging and treatment of cancer. We hypothesized that the disulfide bond of Doxo-SS-Gd-DTPA will be cleaved by GSH enzyme, when it enters into the cancer cells. After cleavage, Doxo and Gd-DTPA will be released, where Doxo will lead to killing the cells and Gd-DTPA will act as T1 MR bright contrast. Along with the contrast and anticancer property, we introduced folate surface functionality, which would help in specifically targeting cancer cells. Further, the probe will remain inactive (prodrug) when it is in the blood stream because the level of the GSH is lower (1-10 μM) in the blood stream; and it is high in the cancer cells (1-10 mM) So, the same probe in the cancer cells get cleaves and releases the Doxo and Gd-DTPA (**Scheme 5B**).

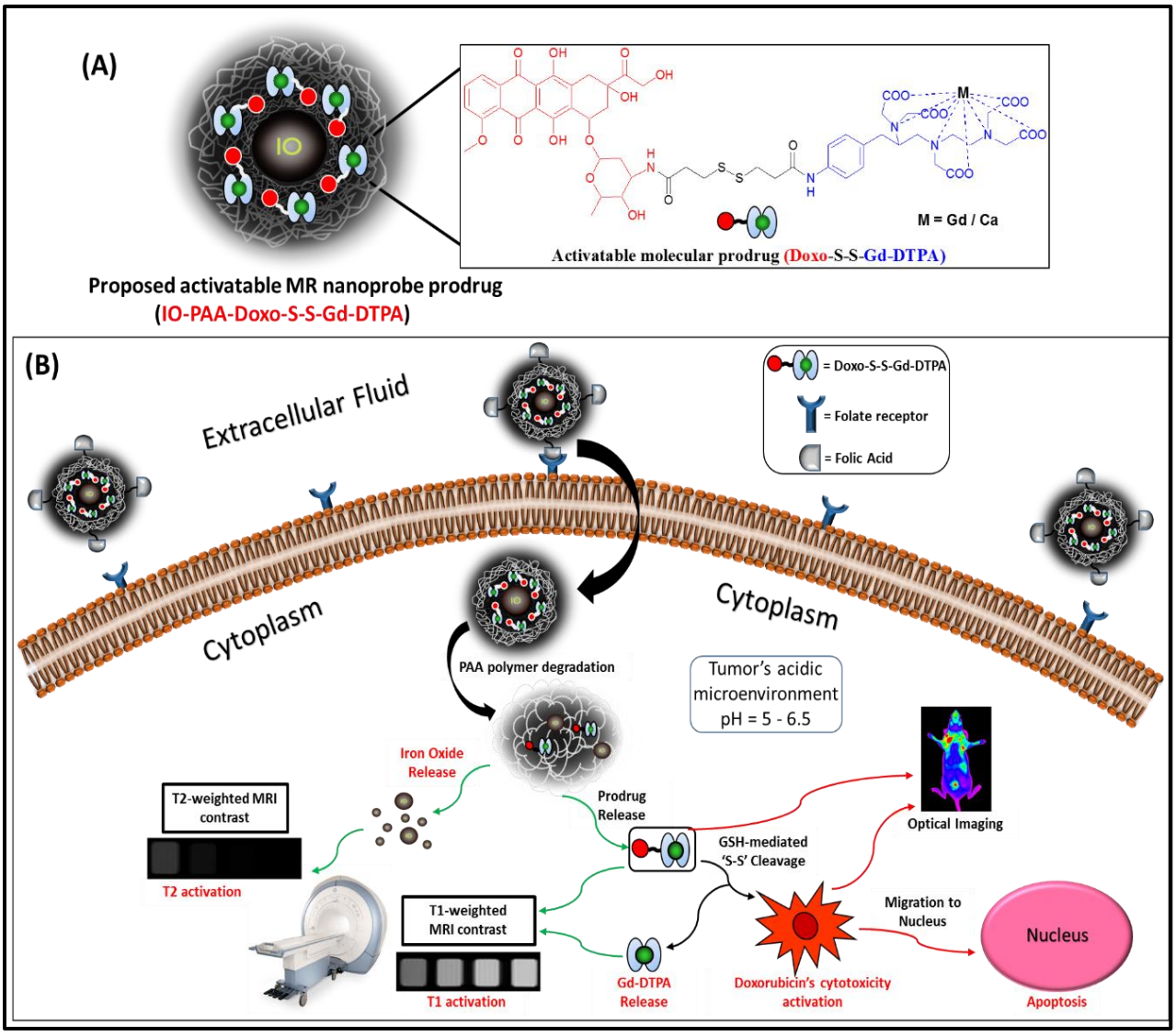

Scheme 5: (A) The representation of the proposed activatable MR nanoprobe-prodrug. (B) Schematic diagram of the mechanism of action T1 and T2 MR activation, and pro-drug activation.

CHAPTER II

RESULT AND DISCUSSION

In this study, we introduced a new cleavable Doxo-SS-Gd-DTPA prodrug; which will be used as a therapeutic agent in conjunction with T1 and T2 imaging for cancer. This prodrug will be encapsulated within PAA polymer coating of IONP-Fol, a typical T2 agent. This would result in the quenching of gadolinium's T1 signal due to the proximity of iron oxide. The folate on the surface of IONP helps in recognition of the cancer cells from the healthy cells because most of the cancer cells overexpress folate receptors. Thereby, the prodrug is targeted to the tumor site. However, upon target recognition, the PAA coating will be disrupted by the tumor's low pH microenvironment, followed by the prodrug Doxo-SS-Gd release. In addition, the released prodrug will be exposed to higher GSH level in the cytosol, which will cleave Doxo and Gd-DTPA complex from the Doxo-SS-Gd-DTPA prodrug. This would lead to an enhanced toxicity from Doxo and activatable T1 MR signal from the Gd-DTPA complex. Hence, the proposed system would provide dual-mode MR imaging of cancer, targetability as well treatment for cancer.

Synthesis of DOXO-SS-Gd-DTPA: Doxorubicin and Gadolinium in the Doxo-SS-Gd-DTPA complex is useful for treatment and imaging, respectively. Magnetic resonance imaging (MRI) technology is often implemented in the clinical diagnosis of illnesses and animal imaging [8].

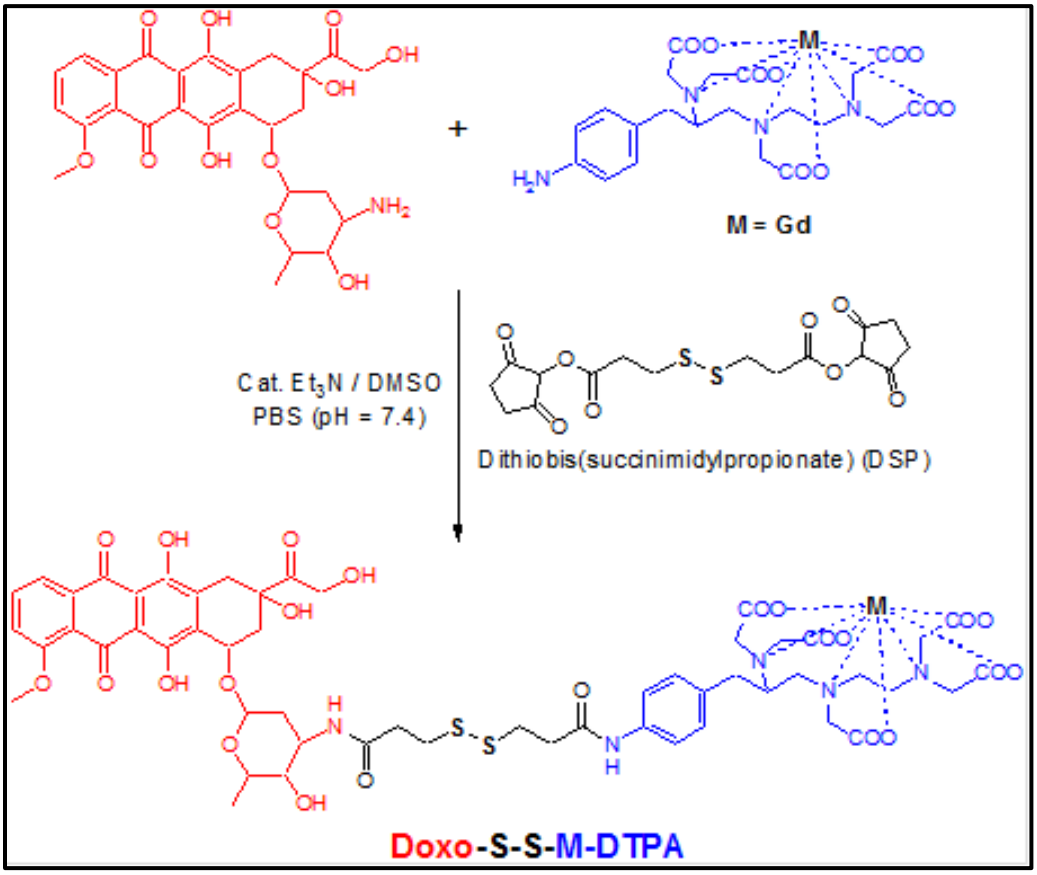

Scheme 6: The synthesis and the mechanism of the activatable prodrug.

The Gd-DTPA complex was synthesized using reported protocol[8] prior to the molecular probe synthesis (Doxo-SS-Gd-DTPA), and dissolved in water. T1 and T2 MR values were measured and dilution was carried out until desired T1 and T2 values were achieved. Furthermore, Doxo was conjugated to Gd-DTPA complex using DSP cross-linker. The NH_2 group on Gd-DTPA complex and Doxo

gets attached to the DSP linker in presence of Et_3N in order to synthesize activatable Doxo-SS-Gd-DTPA complex in solution (**Scheme 6**). When this probe will enter the cancer cells the S-S bond will break due to a high level of glutathione in cancer cells. This solution was further characterized and then encapsulated in IONP.

Characterization of Doxo-SS-Gd-DTPA: After preparation of Doxo-SS-Gd-DTPA solution, the absorbance and fluorescence intensity were measured for detecting the presence of Doxo. An absorbance peak for the free Doxo and free molecular Doxo-SS-Gd-DTPA probe was detected at 495 nm (**Figure A**). Although there was a slight decrease in the intensity of free molecular probe, the absorbance wavelength was similar to that of free Doxo. After measuring the absorbance, the fluorescence intensity was also measured for both free Doxo and free molecular probe which was at 595 nm (**Figure B**). Again, there was a slight decrease in the intensity of free molecular probe because Doxo is complexed with Gd-DTPA.

Moving forward, T1 and T2 values were taken for the same sample; T1 value was measured to be 53.43 ms (**Figure C**) which is a very strong signal for T1, whereas T2 was 700 ms (**Figure D**) indicative of the weak T2 MR property of the molecular probe.

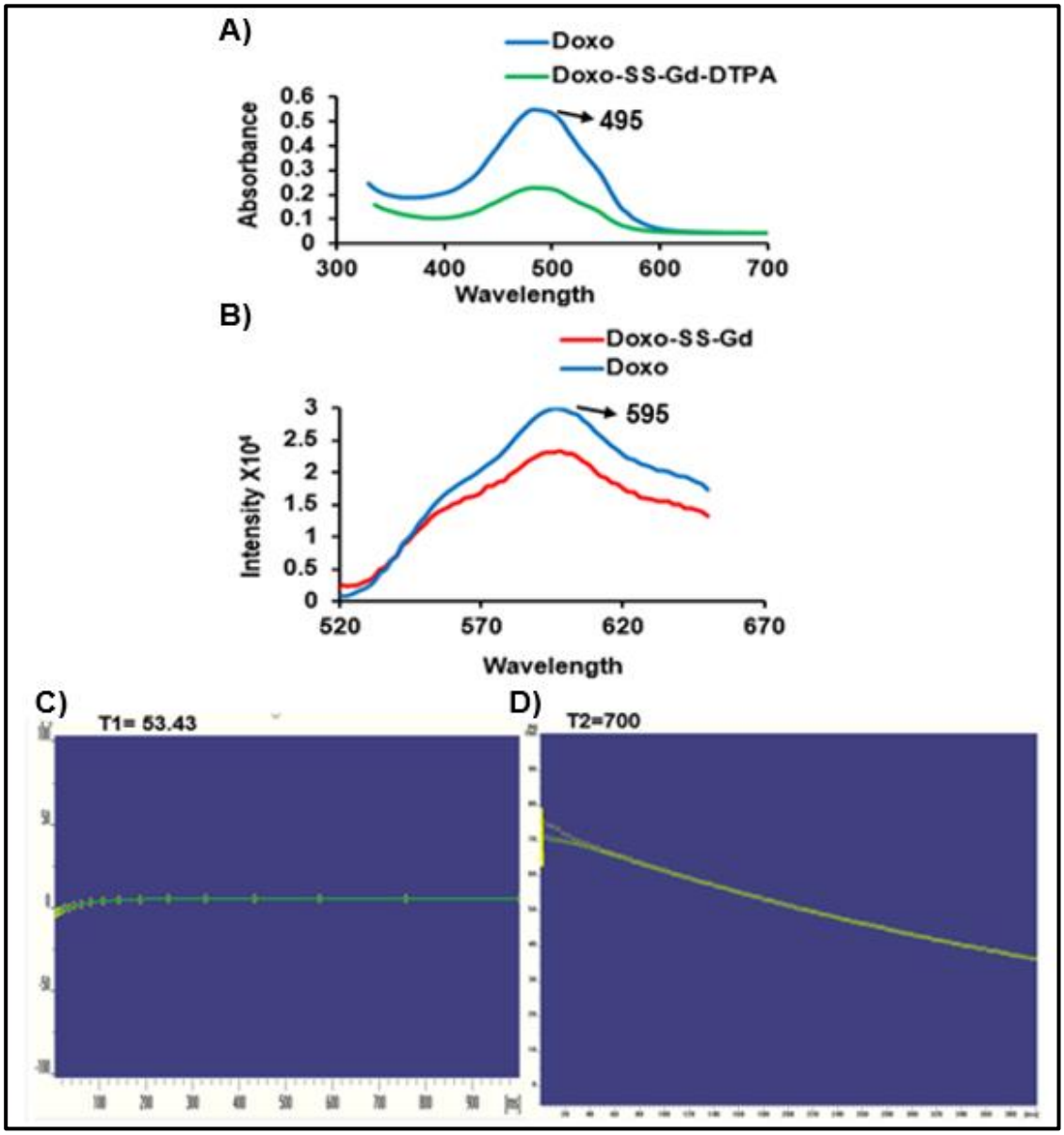

Figure 2: (A) Comparison between free Doxo and the molecular probe UV. (B) Comparison between free Doxo and the molecular probe fluorescence. (C), (D) MR Data of molecular probe before encapsulation.

Synthesis of iron oxide nanoparticles (IONP): Iron oxide nanoparticles (IONP) has attracted large interest due to their superparamagnetic property. Some common uses of synthesized nanoparticles include high-sensitivity bimolecular MRI, catalysis, superparamagnetic relaxometry (SPMR), and sensors[20]. Herein, we formulated iron oxide nanoparticle using solvent precipitation method. For performing the synthesis of IONP, three different solutions of i) iron salts solution, ii) poly acrylic acid (PAA) solution, and iii) ammonium hydroxide (NH_4OH) solution were prepared. First, the iron salts solution was added to NH_4OH solution with constant mixing using vortex, and then PAA solution was added to stabilize the iron oxide nanoparticles. After carrying out the entire reaction, the resultant IONP solution was centrifuged to bring it to the desired size. Further, the solution was purified using dialysis technique and characterized using DLS (dynamic light scattering).

Molecular and nano prodrug	T1 (ms)	T2 (ms)
Doxo-SS-Gd	53.43	700
Doxo-SS-Gd-DTPA-IONP	139	79

Table 1: Molecular probe before encapsulation MR Data and Nanoprobe after encapsulation MR Data.

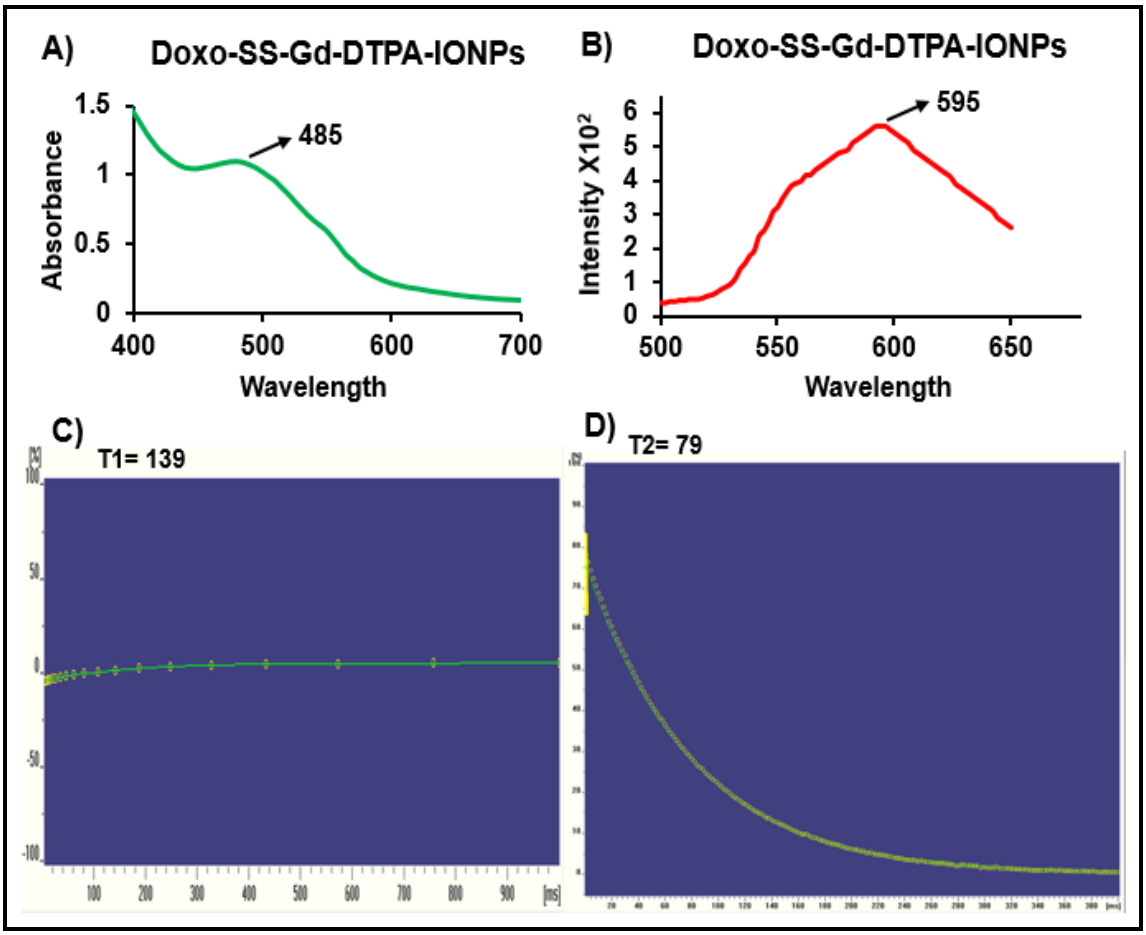

Figure 3: (A) After encapsulation UV for Doxo-SS-Gd-DTPA-IONPs. (B) After encapsulation fluorescence for Doxo-SS-Gd-DTPA-IONPs. (C), (D) Nanoprobe after encapsulation MR Data.

The synthesized Doxo-S-S-Gd-DTPA was also characterized using Bruker's Microflex MALDI-TOF spectrometer using dihydrobenzoic acid as matrix. A detected a peak at 1210 Da, which corresponds to the (M-5H) + peak. It indicates that 5 protons were eliminated from DTPA during the ionization process (**Figure 4**).

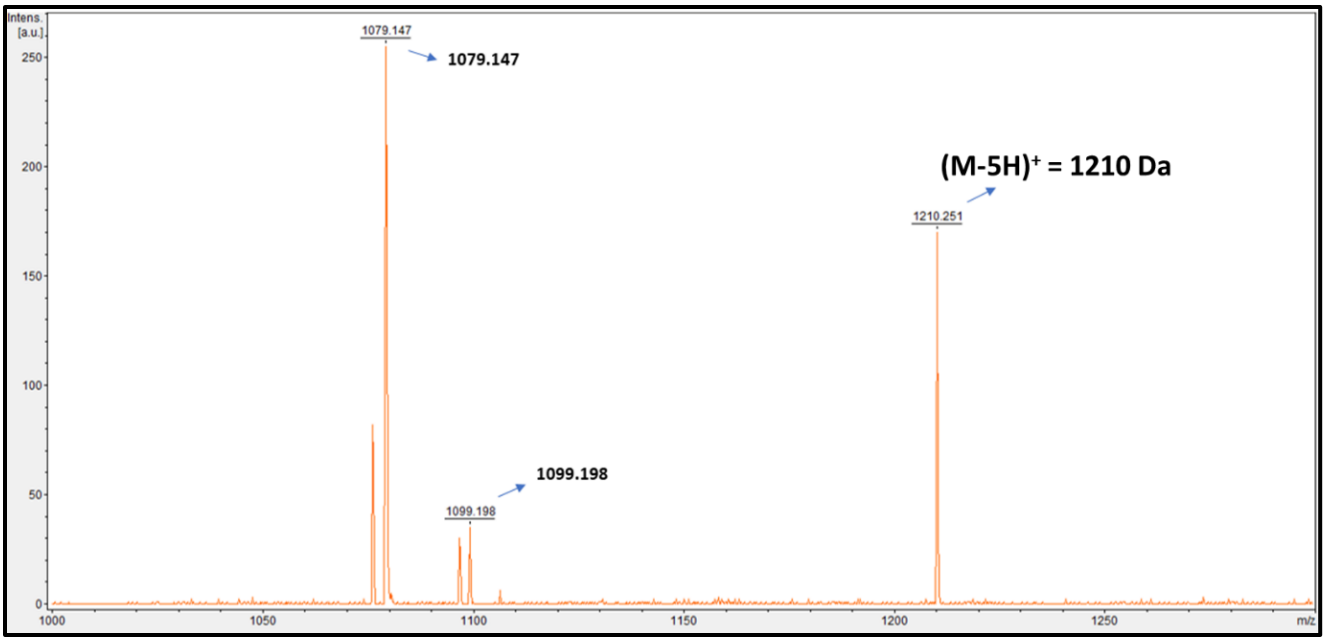

Figure 4: MALDI-TOF spectrum of Doxo-S-S-Gd-DTPA prodrug.

Synthesis of activatable magnetic nanoprobe: After the preparation of IONPs and Doxo-SS-Gd-DTPA solutions, the nanoprobe was formulated. Doxo-SS-Gd-DTPA complex was encapsulated into PAA coatings of IONPs, using solvent diffusion technique. After the encapsulation, pure solution of IONP-PAA-Doxo-SS-Gd-DTPA was obtained by dialysis technique and conjugation with folate was carried out to achieve surface functionality. As most of the cancer cells have folate receptor overexpression, folic acid was used as a targeting ligand for prostate cancer. The functionalization was carried out using EDC/NHS bio conjugation chemistry (**Scheme 7**). First, EDC solution was added to IONP-PAA-Doxo-SS-Gd-DTPA complex followed by addition of NHS and PEG-Folate. Therefore, a solution of IONP-PAA-Doxo-SS-Gd-DTPA-Fol (nanoprobe) was obtained and purified using dialysis. This solution was characterized and used for performing experiments.

Characterization of Functional nanoprobe: Post encapsulation within IONPs was characterized using UV/Vis and fluorescence measurement, which shows peaks at 485 and 495, respectively. These values were similar to what we observed prior to encapsulation, indicating that there is no major change in the characteristics after encapsulating Doxo-SS-Gd-DTPA complex in the IONPs. To check the magnetic property of the nanoprobe, we quantified MR signals which were found to be 139 ms and 79 ms of T1 and T2 values individually (**Table 1**). The reason for the change in T1 and T2 before and after encapsulation is because this T1 MR activatable prodrug's signal would be (Doxo-SS-Gd-DTPA) quenched in presence of IONP (strong T2 agent). However, when the prodrug enters the body a strong T1 signal could be noticeable only in the acidic microenvironment of tumor where it gets activated.

Furthermore, the presence of folate on the surface after conjugation was detected by UV Vis and fluorescence. The absorbance wavelength was λ_{abs} = 365 nm and the fluorescence was λ_{em} = 452 nm after surface conjugation with folate (**Figure 5D & B**). The wavelength of absorbance and fluorescence intensity were comparative to that of free folic acid depicting there is no change in the characteristics of folate after conjugation. (**Figure 5A & C**).

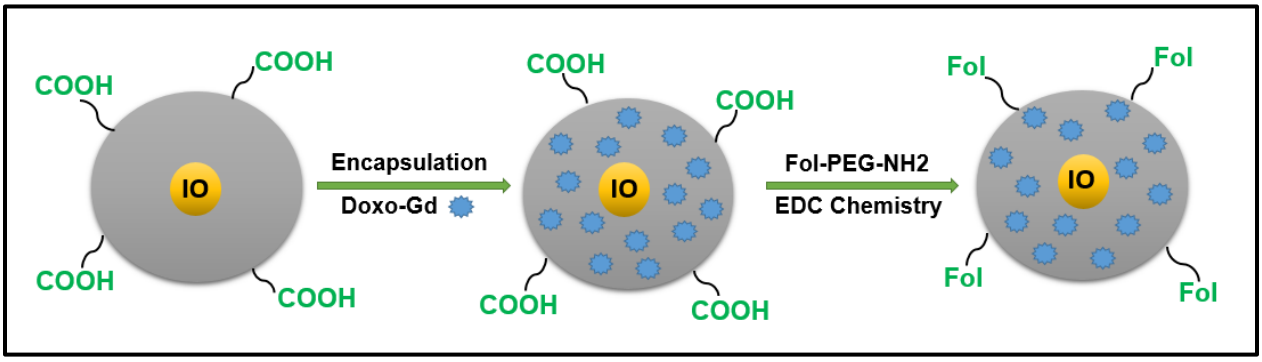

Scheme 7: Surface conjugation of Fol-PEG-NH_2 on the IONPs using EDC/NHS chemistry.

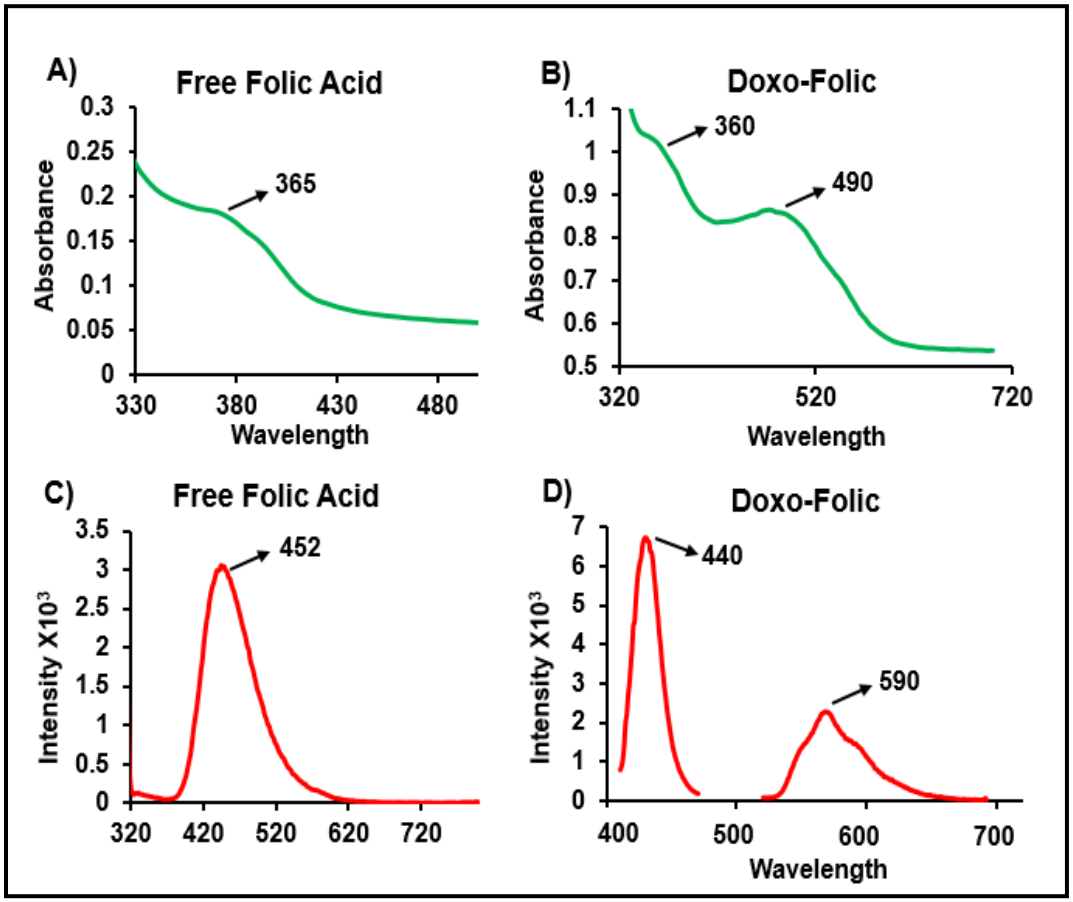

Figure 5: Surface conjugation with folate UV (A) Free folic acid, (B) Doxo-Fol. Surface conjugation with folate Fluorescence (C) Free folic acid, (D) Doxo-Fol fluorescence.

Characterization studies: The hydrodynamic size and zeta potential of IONP-COOH, Doxo-SS-Gd-IONPs, and Doxo-SS-Gd-IONPs-Fol were determined with the help of DLS. According to the results (**Figure 6**), the size of IONP-COOH was noted to be 66.57 nm, while Doxo-SS-Gd-IONPs size was increased to 72.26 nm due to its encapsulation. After folate conjugation on the surface of Doxo-SS-Gd-IONPs, the hydrodynamic diameter was amplified to 75.91 nm. Increase in size portrays the presence of a huge functional group on the surface. Zeta potential of the solutions was also determined along with the hydrodynamic diameter. The surface zeta potential of IONP-COOH was noted to be -32.7 mV because of the negativity of -COOH group. Whereas, the surface charge for Doxo-SS-Gd-IONPs was determined to be -26.6 mV and that of nanoprobe conjugated with the folate had a zeta potential of -38.4 mV. Hence, the change in zeta potential before and after conjugation depicts the successful conjugation of folate on the surface of IONP-COOH.

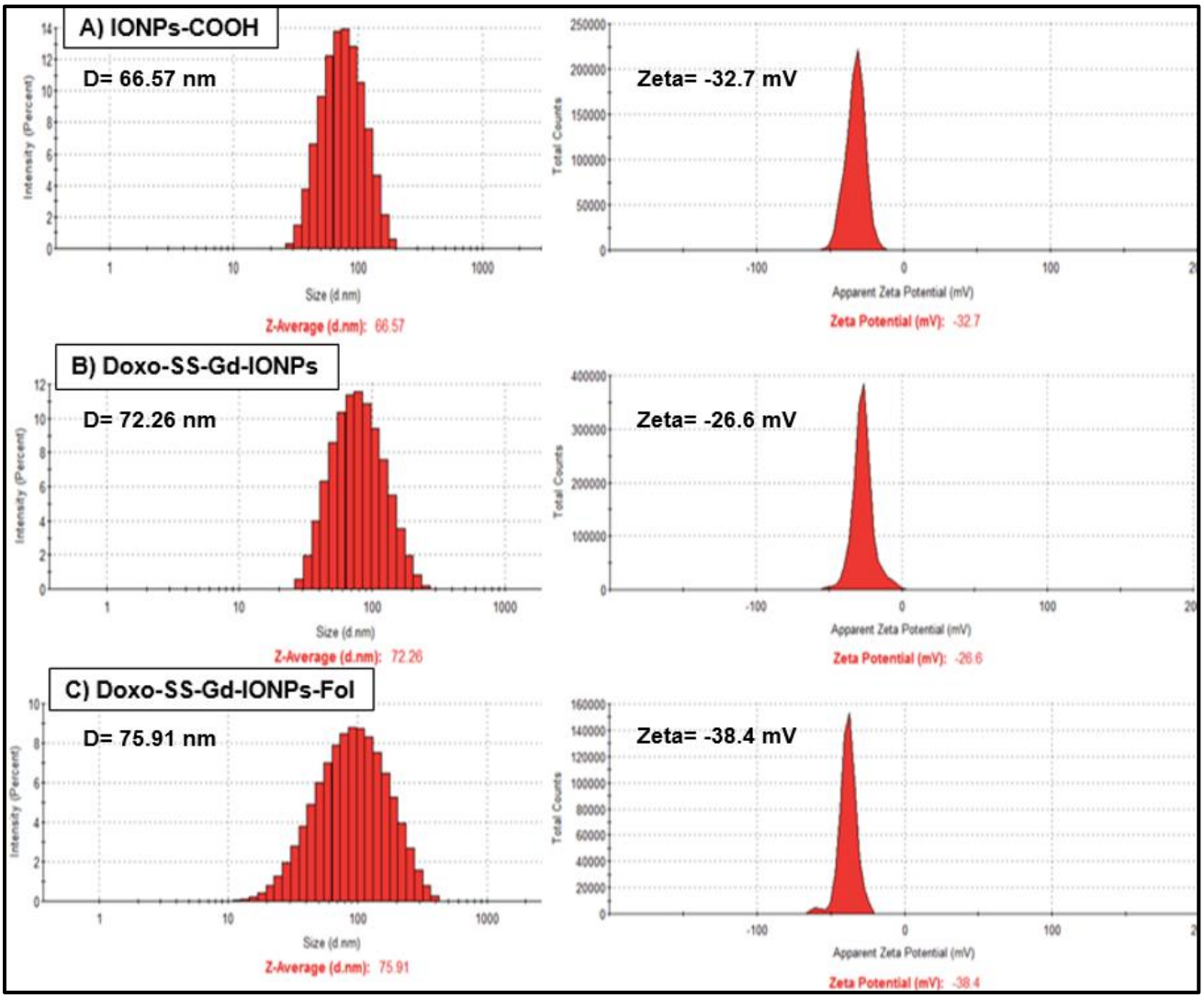

Figure 6: Determination of size and zeta potentials of the functional nanoprobes.

In-vitro Cell viability (MTT assay): MTT assay is a colorimetric assay which helps to find out the cytotoxicity of drug by determining the cell viability. In the presence of mitochondrial reductase of healthy cells, MTT solution turns to formazan crystals (purple colored compound). The yellow colored MTT solution when added to the nanoprobe treated cells changes to purple color indicating the cells viability. Depending on the density of the color, we could determine how

many cells are viable. In here, we used this cell based assay in determining the cytotoxicity of IONP-Doxo-SS-Gd-DTPA probe on LNCaP cells. Different time points were selected for conducting the experiment. Initially, we seeded the cells in a 96 well plate and then treated them with different composition of nanoprobe encapsulated in IONPs. As see in (**Figure 7**)**,** after 24 h treatment, IONP-Doxo-SS-Gd-DTPA-Fol show 60 % cell viability whereas IONP-Doxo-Fol have 70 % cell viable. When relating this result with IONP-Gd-DTPA-Fol, it has 80% cells viable showing minimal cytotoxic effect. The cytotoxicity study at 36 h displayed the cell viability after treatment with IONP-Doxo-SS-Gd-DTPA-Fol was as low as 35% whereas with IONP-Doxo-Fol was approximately 40%, which was fairly close to the cytotoxicity value of the former.

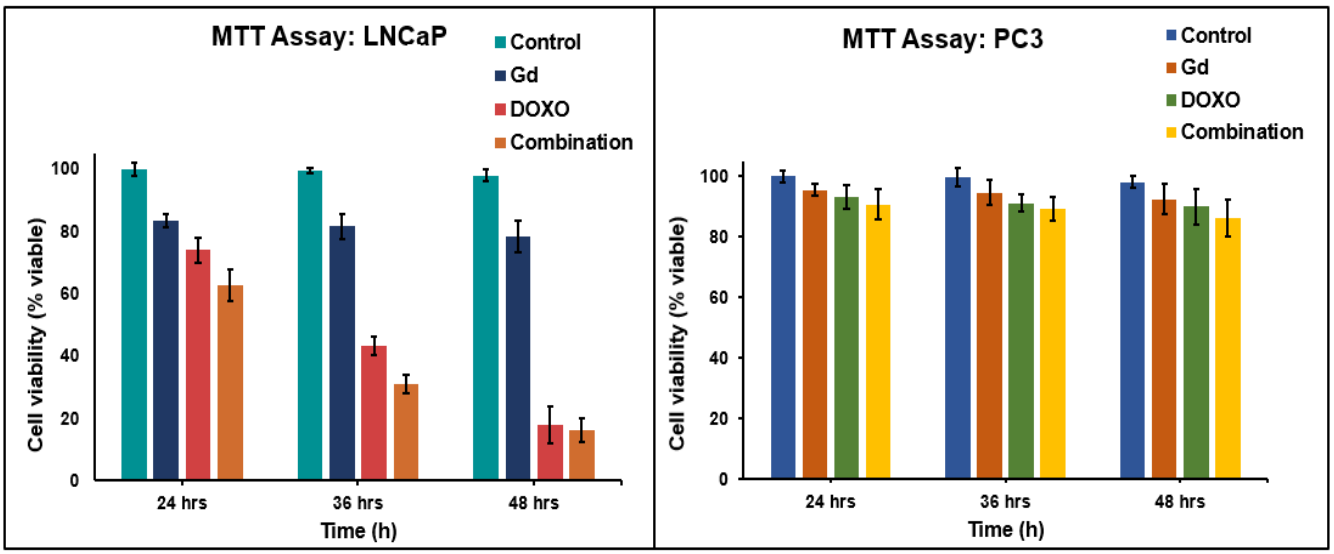

Figure 7: Cellular toxicity of the nanoprobe using LNCaP cells and PC3 cells.

The cell viability after treating with IONP-Gd-DTPA remained pretty constant proving that it does not play a major role in the cytotoxicity. At 48 h, treatment with IONP-Doxo-SS-Gd-DTPA-Fol resulted in the viability to be least, suggesting maximum cell death. Similar cytotoxicity was also observed with IONP-Doxo-Fol while IONP-Gd-DTPA-Fol showed very low cytotoxicity. Conclusively, IONP-Doxo-SS-Gd-DTPA-Fol probe was effective in killing the cancer cells over time. As a negative control, the same assay was performed on PC-3 cells and the viability of cells were found to be consistent at all-time points. This indicates that the nanoprobe designed was specific to LNCaP cells.

Cell Internalization Studies: Following the MTT assay, the nanoprobes ability to enter the cancerous cells were visually determined by performing cellular uptake study. After 12 h of treatment with the nanoprobe **(Figure 8A-D)**, we observed cytoplasm was stained red due to the fluorescence effect of Doxo whereas the nucleus was stained blue with DAPI dye suggesting the internalization of nanoprobes into the LNCaP cells. As in **Figure 8E-L,** at 24 h and 48 h, the amount of cell viability decreased drastically indicating the cytotoxic effect of Doxo on LNCaP. When similar cell uptake study was done with PC-3 cells, there was negligible entry of the nanoprobe proving the specificity of the nanoprobe to LNCaP cells as in **figure 8M-P**.

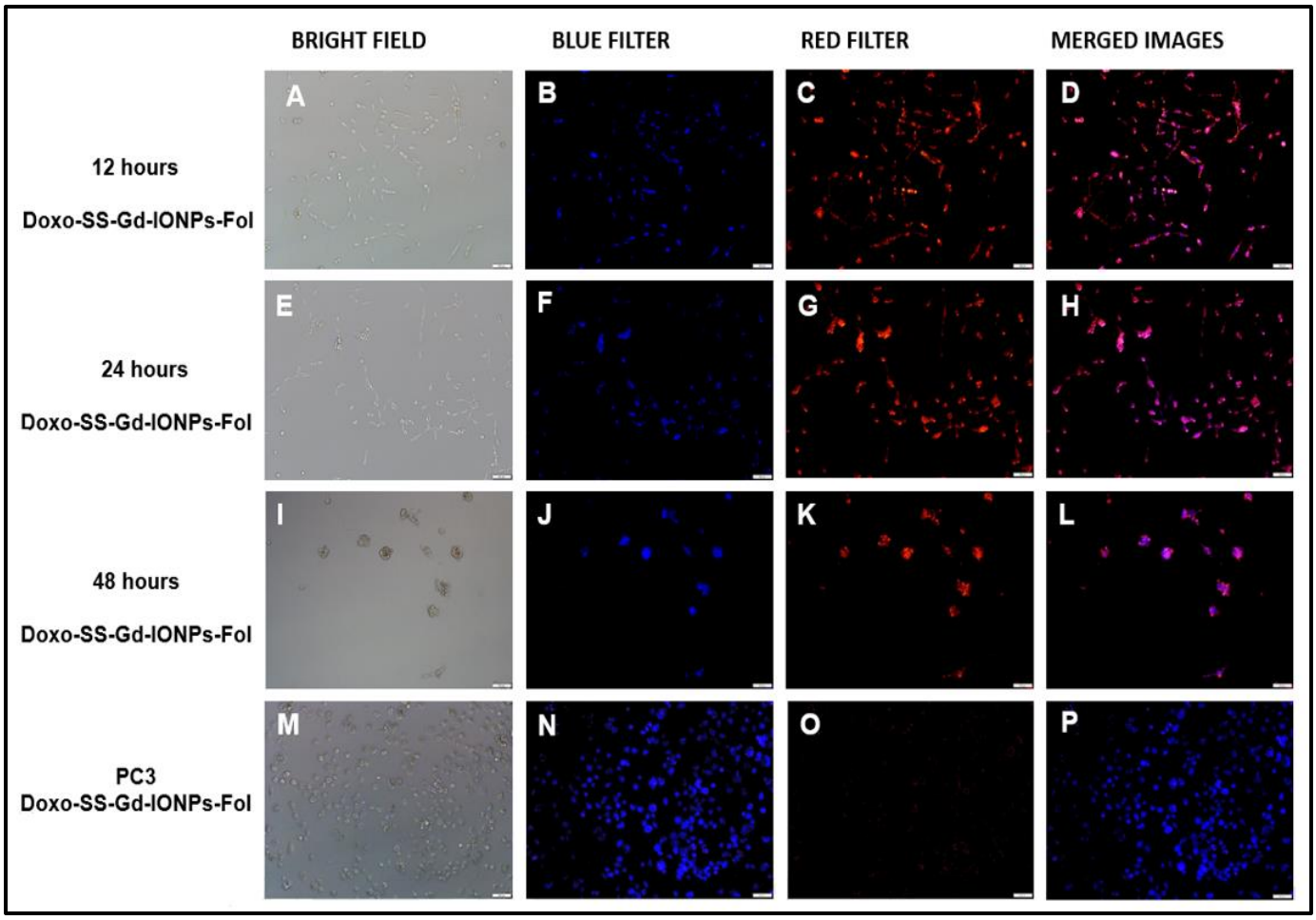

Figure 8: Cellular toxicity and viability of MR activatable nanoprobe.

We performed activation study at different pH for different concentration of Gd encapsulated in nanoprobe at 0 h and 24 h. We can notice from **Figure 9** that increase in Gd concentration, Δ1/T1 value was increased and maximum T1 MR activation was observed at pH 4.0-5.0. This also indicated that the signal is directly proportional to the concentration and related to change in pH. Parallelly, Δ1/T2 value was plotted for different concentration of Fe at different pH and found that there was minimal change in T2 MR signal between these different

groups. In conclusion, the synthesized nanoprobe was T1 MR activatable and cytotoxic *in vitro*.

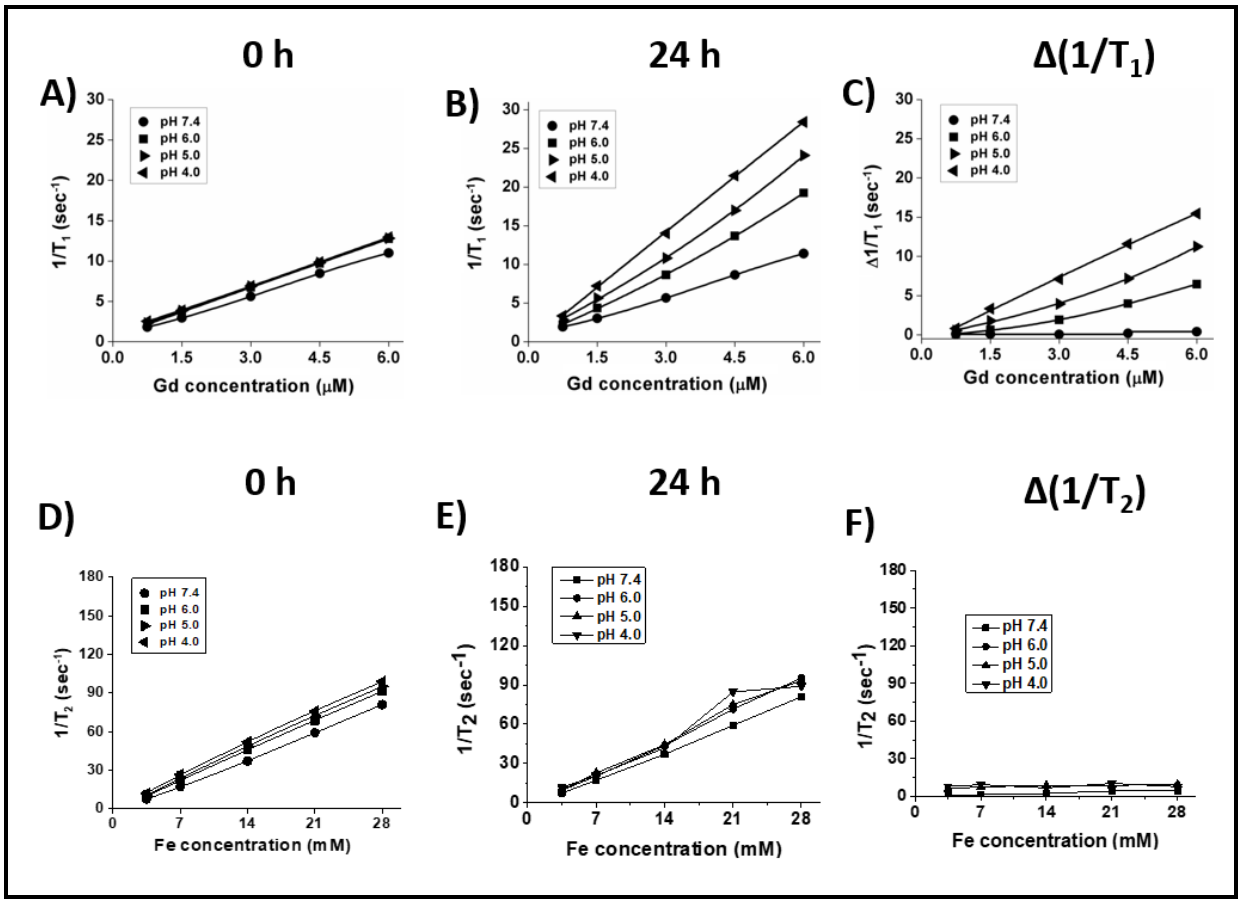

Figure 9: Evaluation of magnetic activation of Doxo-SS-Gd-DTPA-IONPs-Fol using Bruker's magnetic relaxometer.

MRI-Based T1-Weighted Activation of the Composite Nanoprobe: We studied if the observed pH-dependent increases in R1 (1/T1) of the nanoprobe results leads to increases in the T1-weighted signal in MRI, which leads to an increase in the brightness of the image. This would be one-step closer to the application of our nanoprobe for the cancer imaging application. For this, we took the different concentrations of our prodrug encapsulating IONPs and used 9T clinical MRI instrument for the T1 and T2 MR scanning at pH 5.0 (**Figure 10**).

The T1-weighted MR signals were increased as the concentrations of the activatable nanoprobes increase (from 0.75 to 6.0 μM of Gd), which reflected in the increase in T1 signals of the corresponding MR images (**Figure 10A**). This is indicative of the T1 MR signal activation at the lower pH. However, the T2 MR signal was not quenched, rather the images were darker as the iron concentrations increased (**Figure 10B**).

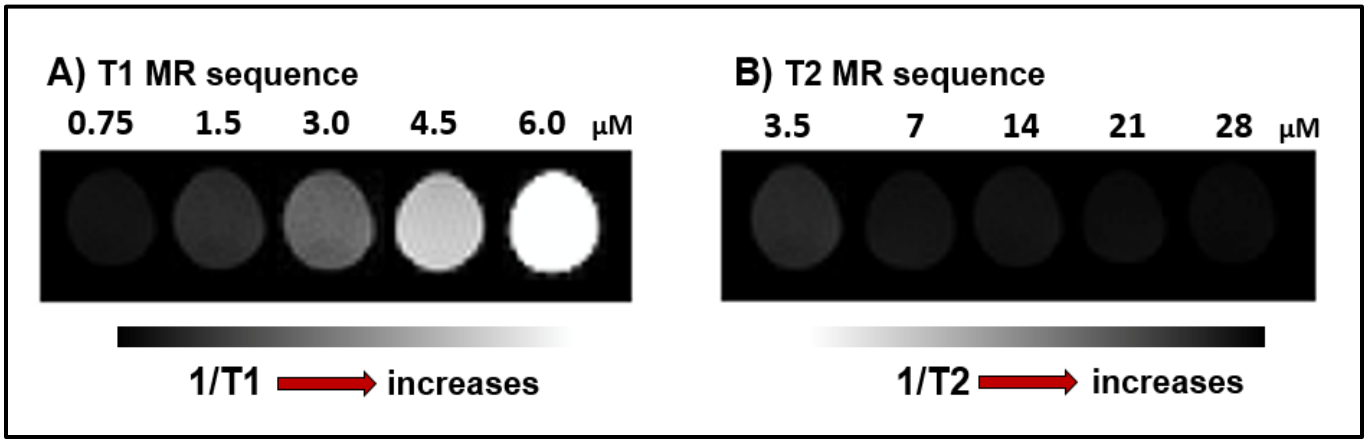

Figure 10: Magnetic resonance imaging (MRI) studies measuring the T1 MR activation in PBS, pH 5.0 using Bruker's 9T clinical MRI instrument.

CHAPTER III

METHODS AND EXPERIMENTAL SECTION

Synthesis of PAA coated IONPs: Iron oxide nanoparticles (IONPs) coated with PAA were synthesized using “water-based precipitation method”. To synthesize PAA coated IONPs, three solutions were prepared: i) Iron salts solution (0.7 g of $FeCl_3$.6 H_2O and 0.4 g of $FeCl_2$ .4H_2O in 100 µL of 12 N HCl and 2 mL of DI H_2O), ii) an alkaline solution (1.8 mL of 30% NH_4OH solution in 15 mL of deionized water) and iii) stabilizing agent solution (2 g of PAA in 5 mL of DI water). The synthetic procedure was as follows: The solution of iron salts was added into alkaline solution. Afterwards, stabilizing agent (PAA in DI water) was added to the above solution and the reaction was continued at a speed of 4000 rpm. Then, the resulting IONPs were centrifuged at 3000 rpm, 4000 rpm and 4000 rpm for 20 min each, respectively. The supernatant obtained after the final centrifugation was dialyzed in a dialysis bag, which has a molecular weight cut off range of 6-8 kDa. The dialysis process was done in beaker with DI water and a magnetic stirrer. The water was changed periodically for 24 h and the dialyzed IONPs were taken out of dialysis bag, labelled and stored.

Synthesis of the Gd-DTPA: Gd-DTPA is a highly stable paramagnetic complex which was synthesized by adding a solution of gadolinium chloride hexahydrate ($GdCl_3.6H_2O$) in a solution of diethylenetriaminepentaacetic acid (DTPA). 4.49 g of $GdCl_3.6H_2O$ was dissolved in 10 mL of deionized water to make a molar concentration of 0.0121 M. Then, DTPA of 5.0 g was dissolved in 30 mL of water containing 2 N NaOH (5.0 mL) solution to form 0.0127 M solution of DTPA. These prepared stock solutions of gadolinium and DTPA were mixed together by dropwise addition of $GdCl_3.6H_2O$ solution to DTPA solution. Thereafter, 2 N NaOH was continuously added to the above solution to bring the pH to 6.8 and the reaction was maintained at 80°C for 12 h. This reaction led to the formation of white crystals which were initially dissolved little amount of water followed by precipitation with ethanol. Once precipitated the solution was filtered to remove the Gd-DTPA complex and dried under vacuum

Encapsulation of Gd-DTPA-IONPs: In a 15 mL tube, we took 5 mL of the freshly prepared IONP and then we added 500 µL of Gd-DTPA drop by drop at 1200 rpm on vortex mixer. It was allowed to mix in the orbital mixer overnight and then T1 and T2 values were detected.

Synthesis of Doxo-SS-Gd-DTPA: Doxorubicin hydrochloride salt was made into an aqueous solution and added to PBS buffer solution of pH 7.4 to form amine free doxorubicin. This was allowed to centrifuge and the supernanant was removed. The solid pellet from the centrifugate was dissolved in dimethyl sulfoxide (DMSO) forming doxorubicin solution. 1.84 mM solution of dithiobis (succinimidyl propionate) (DSP) was added dropwise to a mixture containing solution of Gd-

DTPA complex solution and doxorubicin solutions. To this above mixture, a small amount of triethylamine (0.4 µL in DMSO) was added at 25°C for 30 mins, followed by incubation overnight at 4°C. The synthesized probe was finally characterized using various spectroscopic methods including MALDI-TOF.

MALDI Matrix Preparation:

1. Preparation of TA30 Solvent:

   TA30 is a 30:70 (vol/vol) mixture of acetonitrile (ACN): trifluoroacetic acid (TFA) in deionized water. First, the acid solution was diluted, then combined with 300 µL AcN + 699.3 µL deionized water + 0.7 µL TFA = 1 mL TA30.

2. Matrix Solubilization:

   Add 2, 5-Dihydroxybenzoic acid (20 mg/mL) to the TA3O solution and vortex until dissolved.

3. Sample Preparation:

   Nanoprobe was dissolved in methanol of 50 mg/mL.

4. Sample Plating:

   Equal volumes of matrix solution and nanoprobe solution were taken into a new tube and vortexed for a few minutes until thoroughly mixed. Then, 0.5 µL drop of this solution was placed on the MALDI plate. The sample was allowed to completely air dry in the hood overnight.

Cytotoxicity assay (MTT): For estimating the toxicity of the nanoprobe, MTT assay was performed. LNCaP cells were seeded on a 96 well plate for 24 hours and stored at 37°C. On the next day, they were treated with IONP-Gd-Fol, IONP-DOXO-Fol and IONP-Doxo-SS-Gd-DTPA-Fol, which was incubated for 12, 24, 36 and 48 hours. Following the respective treatment period, 30 µL MTT solution was added in each well and again stored for 4-6 hours. This helped in formation of purple formazan crystals which could help us in determining the live cells. To dissolve the purple color formazan, acidic isopropyl solution was added and kept on thermo-mixture overnight. Finally the fluorescence was measured at 570 nm using a plate reader and results were plotted.

Magnetic relaxation: Magnetic relaxation of different samples were performed at KUMC and images were obtained.

CHAPTER IV

CONCLUSION

We designed and synthesized an activatable doxorubicin-based prodrug Doxo-S-S-Gd-DTPA and characterized it using various spectroscopic methods. This prodrug was encapsulated in PAA-coated IONPs and characterized. The IONP-PAA-Doxo-SS-Gd-DTPA-Fol nanoprobe, which quenches T1 signal (low Δ1/T1), when at close vicinity to the strong T2 agent IONP. Upon release of Doxo-SS-Gd-DTPA from the nanoprobe complex, Δ1/T1 was increased indicating quenching effect. This release of the T1 agent from the IONP-based nanoprobe complex leads to improved MRI contrast. Though the release of the Doxo-SS-Gd-DTPA altered T1 signal, it had only minimal effect on T2 signaling.

Next, we performed cell uptake study in order to assess the specificity of the nanoprobe to the LNCaP cells, which targeted only cancerous cells because of the functionalization with folate on the IONPs. Once internalized, the nanoprobe complex was dissociated due to the presence of glutathione, where Doxo-complex enhanced cytotoxic effect and Gadolinium-complex was helpful in MR imaging. To assess the cytotoxic capability of the nanoprobe MTT assay was performed, which showed that after nanoprobe treatment less viable cells were present at 48 h. The activation study was performed which presented that the

activation of nanoprobe varied with concentration and pH, showing maximum activation taking place at relatively higher concentration and lower pH.

REFERENCES

(1) Cancer Facts and Statistics. (n.d.). Retrieved from https://www.cancer.org/research/cancer-facts-statistics.html.

(2) Nguyen, K. T. (2011). Targeted nanoparticles for cancer therapy: promises and challenge.

(3) Gupta, A. K., & Gupta, M. (2005). Synthesis and surface engineering of iron oxide nanoparticles for biomedical applications. *Biomaterials*, *26*(18), 3995-4021.

(4) Hu, X., & Norris, D. G. (2004). Advances in high-field magnetic resonance imaging. *Annu. Rev. Biomed. Eng.*, *6*, 157-184.

(5) Santra, S., Jativa, S. D., Kaittanis, C., Normand, G., Grimm, J., & Perez, J. M. (2012). Gadolinium-encapsulating iron oxide nanoprobe as activatable NMR/MRI contrast agent. *ACS nano*, *6*(8), 7281-7294.

(6) Gole, A., Stone, J. W., Gemmill, W. R., zur Loye, H. C., & Murphy, C. J. (2008). Iron oxide coated gold nanorods: synthesis, characterization, and magnetic manipulation. *Langmuir*, *24*(12), 6232-6237.

(7) Huang, J., Wang, L., Lin, R., Wang, A. Y., Yang, L., Kuang, M., & Mao, H. (2013). Casein-coated iron oxide nanoparticles for high MRI contrast enhancement and efficient cell targeting. *ACS applied materials & interfaces*, *5*(11), 4632-4639.

(8) Mahmoudi, M., Simchi, A., Imani, M., & Hafeli, U. O. (2009). Superparamagnetic iron oxide nanoparticles with rigid cross-linked polyethylene glycol fumarate coating for application in imaging and drug delivery. *The Journal of Physical Chemistry C*, *113*(19), 8124-8131.

(9) Lai, J., Shafi, K. V., Ulman, A., Loos, K., Yang, N. L., Cui, M. H., ... & Locke, D. C. (2004). Mixed iron− manganese oxide nanoparticles. *The Journal of Physical Chemistry B*, *108*(39), 14876-14883.

(10) Zhong, Z. Y., Prozorov, T., Felner, I., & Gedanken, A. (1999). Sonochemical synthesis and characterization of iron oxide coated on submicrospherical alumina: a direct observation of interaction between iron oxide and alumina. *The Journal of Physical Chemistry B*, *103*(6), 947-956.

(11) Xu, Y., Qin, Y., Palchoudhury, S., & Bao, Y. (2011). Water-soluble iron oxide nanoparticles with high stability and selective surface functionality. *Langmuir*, *27*(14), 8990-8997.

(12) Wang, X., Krommenhoek, P. J., Bradford, P. D., Gong, B., Tracy, J. B., Parsons, G. N., ... & Zhu, Y. T. (2011). Coating alumina on catalytic iron oxide nanoparticles for synthesizing vertically aligned carbon nanotube arrays. *ACS applied materials & interfaces*, *3*(11), 4180-4184.

(13)Santra, S., Kaittanis, C., Santiesteban, O. J., & Perez, J. M. (2011). Cell-specific, activatable, and theranostic prodrug for dual-targeted cancer imaging and therapy. *Journal of the American Chemical Society*, *133*(41), 16680-16688.
(14)Ogawa, M., Kosaka, N., Longmire, M. R., Urano, Y., Choyke, P. L., & Kobayashi, H. (2009). Fluorophore− quencher based activatable targeted optical probes for detecting in vivo cancer metastases. *Molecular pharmaceutics*, *6*(2), 386-395.
(15)Cao, S., Pei, Z., Xu, Y., & Pei, Y. (2016). Glyco-nanovesicles with activatable near-infrared probes for real-time monitoring of drug release and targeted delivery. *Chemistry of Materials*, *28*(12), 4501-4506.
(16)Zheng, M., Wang, Y., Shi, H., Hu, Y., Feng, L., Luo, Z., & Ye, D. (2016). Redox-mediated disassembly to build activatable trimodal probe for molecular imaging of biothiols. *ACS nano*, *10*(11), 10075-10085.
(17)Perez, J. M., & Santra, S. (2014). *U.S. Patent Application No. 13/936,933*.
(18)Rathinaraj, P., Lee, K., Park, S. Y., & Kang, I. K. (2015). Targeted images of KB cells using folate-conjugated gold nanoparticles. *Nanoscale research letters*, *10*(1), 5.
(19)Yang, C. T., Padmanabhan, P., & Gulyás, B. Z. (2016). Gadolinium (iii) based nanoparticles for T 1-weighted magnetic resonance imaging probes. *RSC Advances*, *6*(65), 60945-60966.
(20)Mahmoudi, M., Sant, S., Wang, B., Laurent, S., & Sen, T. (2011). Superparamagnetic iron oxide nanoparticles (SPIONs): development, surface modification and applications in chemotherapy. *Advanced drug delivery reviews*, *63*(1-2), 24-46.
(21)Santra, S., Kaittanis, C., Grimm, J., & Perez, J. M. (2009). Drug/dye-loaded, multifunctional iron oxide nanoparticles for combined targeted cancer therapy and dual optical/magnetic resonance imaging. *Small*, *5*(16), 1862-1868.
(22)Yu, C. H., Al-Saadi, A., Shih, S. J., Qiu, L., Tam, K. Y., & Tsang, S. C. (2008). Immobilization of BSA on silica-coated magnetic iron oxide nanoparticle. *The Journal of Physical Chemistry C*, *113*(2), 537-543.
(23)Sulthana, S., Banerjee, T., Kallu, J., Vuppala, S. R., Heckert, B., Naz, S., & Santra, S. (2017). Combination therapy of NSCLC using Hsp90 inhibitor and doxorubicin carrying functional nanoceria. *Molecular pharmaceutics*, *14*(3), 875-884.
(24)Dewi, M. K., Arsianti, A., Zagloel, C. R. Z., Aziza, Y. A. N., Kurniasari, K. D., Mandasari, B. K. D., ... & Putrianingsih, R. (2018). In vitro Evaluation of Seaweed Gracilaria verrucosa for Cytotoxic Activity against Cervical HeLa Cells. *Pharmacognosy Journal*, *10*(5).

(25)Mao, Z., Liu, Z., Chen, L., Yang, J., Zhao, B., Jung, Y. M., & Zhao, C. (2013). Predictive value of the surface-enhanced resonance Raman scattering-based MTT assay: a rapid and ultrasensitive method for cell viability in situ. *Analytical chemistry*, *85*(15), 7361-7368.
(26)Gao, H., Liu, C., Jeong, H. E., & Yang, P. (2011). Plasmon-enhanced photocatalytic activity of iron oxide on gold nanopillars. *ACS nano*, *6*(1), 234-240.
(27)Unni, M., Uhl, A. M., Savliwala, S., Savitzky, B. H., Dhavalikar, R., Garraud, N., & Rinaldi, C. (2017). Thermal decomposition synthesis of iron oxide nanoparticles with diminished magnetic dead layer by controlled addition of oxygen. *ACS nano*, *11*(2), 2284-2303.
(28)Tong, S., Hou, S., Zheng, Z., Zhou, J., & Bao, G. (2010). Coating optimization of superparamagnetic iron oxide nanoparticles for high T2 relaxivity. *Nano letters*, *10*(11), 4607-4613.
(29)Kim, D. K., Mikhaylova, M., Zhang, Y., & Muhammed, M. (2003). Protective coating of superparamagnetic iron oxide nanoparticles. *Chemistry of Materials*, *15*(8), 1617-1627.
(30)Lam, U. T., Mammucari, R., Suzuki, K., & Foster, N. R. (2008). Processing of iron oxide nanoparticles by supercritical fluids. *Industrial & Engineering Chemistry Research*, *47*(3), 599-614.
(31)Kolosnjaj-Tabi, J., Javed, Y., Lartigue, L., Volatron, J., Elgrabli, D., Marangon, I., & Pellegrino, T. (2015). The one year fate of iron oxide coated gold nanoparticles in mice. *ACS nano*, *9*(8), 7925-7939.
(32)Espinosa, A., Di Corato, R., Kolosnjaj-Tabi, J., Flaud, P., Pellegrino, T., & Wilhelm, C. (2016). Duality of iron oxide nanoparticles in cancer therapy: amplification of heating efficiency by magnetic hyperthermia and photothermal bimodal treatment. *ACS nano*, *10*(2), 2436-2446.
(33)Zhou, Z., Wang, L., Chi, X., Bao, J., Yang, L., Zhao, W., & Gao, J. (2013). Engineered iron-oxide-based nanoparticles as enhanced T 1 contrast agents for efficient tumor imaging. *ACS nano*, *7*(4), 3287-3296.
(34)Boddu, S. H., Vaishya, R., Jwala, J., Vadlapudi, A., Pal, D., & Mitra, A. K. (2012). Preparation and characterization of folate conjugated nanoparticles of doxorubicin using PLGA-PEG-FOL polymer. *Med. Chem*, *2*(4), 68-75.
(35)Rathinaraj, P., Lee, K., Park, S. Y., & Kang, I. K. (2015). Targeted images of KB cells using folate-conjugated gold nanoparticles. *Nanoscale research letters*, *10*(1), 5.
(36)Chen, D., Tang, Q., Xue, W., Xiang, J., Zhang, L., & Wang, X. (2010). The preparation and characterization of folate-conjugated human serum albumin magnetic cisplatin nanoparticles. *Journal of biomedical research*, *24*(1), 26-32.

(37)Mendes, R. G., Bachmatiuk, A., El-Gendy, A. A., Melkhanova, S., Klingeler, R., Büchner, B., & Rümmeli, M. H. (2012). A facile route to coat iron oxide nanoparticles with few-layer graphene. *The Journal of Physical Chemistry C*, *116*(44), 23749-23756.
(38)Basuki, J. S., Duong, H. T., Macmillan, A., Erlich, R. B., Esser, L., Akerfeldt, M. C., & Davis, T. P. (2013). Using fluorescence lifetime imaging microscopy to monitor theranostic nanoparticle uptake and intracellular doxorubicin release. *ACS nano*, *7*(11), 10175-10189.
(39)Cabrera, D., Coene, A., Leliaert, J., Artés-Ibáñez, E. J., Dupré, L., Telling, N. D., & Teran, F. J. (2018). Dynamical magnetic response of iron oxide nanoparticles inside live cells. *ACS nano*, *12*(3), 2741-2752.
(40)Di Corato, R., Gazeau, F., Le Visage, C., Fayol, D., Levitz, P., Lux, F., & Wilhelm, C. (2013). High-resolution cellular MRI: gadolinium and iron oxide nanoparticles for in-depth dual-cell imaging of engineered tissue constructs. *ACS nano*, *7*(9), 7500-7512.
(41)Kashyap, S., Woehl, T. J., Liu, X., Mallapragada, S. K., & Prozorov, T. (2014). Nucleation of iron oxide nanoparticles mediated by Mms6 protein in situ. *Acs Nano*, *8*(9), 9097-9106.
(42)Erogbogbo, F., Yong, K. T., Hu, R., Law, W. C., Ding, H., Chang, C. W., & Swihart, M. T. (2010). Biocompatible magnetofluorescent probes: luminescent silicon quantum dots coupled with superparamagnetic iron (III) oxide. *ACS nano*, *4*(9), 5131-5138.
(43)Chen, Z., Yin, J. J., Zhou, Y. T., Zhang, Y., Song, L., Song, M., & Gu, N. (2012). Dual enzyme-like activities of iron oxide nanoparticles and their implication for diminishing cytotoxicity. *Acs Nano*, *6*(5), 4001-4012.
(44)Sanna, V., Pintus, G., Roggio, A. M., Punzoni, S., Posadino, A. M., Arca, A., & Sechi, M. (2011). Targeted biocompatible nanoparticles for the delivery of (−)-epigallocatechin 3-gallate to prostate cancer cells. *Journal of medicinal chemistry*, *54*(5), 1321-1332.
(45)Low, P. S., Henne, W. A., & Doorneweerd, D. D. (2007). Discovery and development of folic-acid-based receptor targeting for imaging and therapy of cancer and inflammatory diseases. *Accounts of chemical research*, *41*(1), 120-129.
(46)Karandish, F., Haldar, M. K., You, S., Brooks, A. E., Brooks, B. D., Guo, B., & Mallik, S. (2016). Prostate-specific membrane antigen targeted polymersomes for delivering mocetinostat and docetaxel to prostate cancer cell spheroids. *ACS omega*, *1*(5), 952-962.
(47)Anderson, C. F., & Cui, H. (2017). Protease-sensitive nanomaterials for cancer therapeutics and imaging. *Industrial & engineering chemistry research*, *56*(20), 5761-5777.

(48)Arora, J. S., Murad, H. Y., Ashe, S., Halliburton, G., Yu, H., He, J., & Khismatullin, D. B. (2016). Ablative focused ultrasound synergistically enhances thermally triggered chemotherapy for prostate cancer in vitro. *Molecular pharmaceutics*, *13*(9), 3080-3090.
(49)Wang, S., Kim, G., Lee, Y. E. K., Hah, H. J., Ethirajan, M., Pandey, R. K., & Kopelman, R. (2012). Multifunctional biodegradable polyacrylamide nanocarriers for cancer theranostics□ a “see and treat” strategy. *ACS nano*, *6*(8), 6843-6851.
(50)Kaittanis, C., Santra, S., Asati, A., & Perez, J. M. (2012). A cerium oxide nanoparticle-based device for the detection of chronic inflammation via optical and magnetic resonance imaging. *Nanoscale*, *4*(6), 2117-2123.